Nanometer-Scale Aspects of Molecular Ordering in Nanocrystalline Domains at a Solid Interface: The Role of Liquid Crystal−Surface Interactions Studied by STM and Molecule Corrals

D. L. Patrick,[†] V. J. Cee,[‡] M. D. Morse,[§] and T. P. Beebe Jr.*[,§]

Department of Chemistry, Western Washington University, Bellingham, Washington 98225, Department of Chemistry, Harvard University, Cambridge, Massachusetts 02138, and Department of Chemistry, University of Utah, Salt Lake City, Utah 84112

Received: June 25, 1999

Chiral molecular monolayers deposited on a graphite surface in contact with a bulk liquid crystal (LC) droplet showed unexpected long-range morphological correlations between adjacent crystalline domains. These correlations included tendencies for nearby surface domains to exhibit similar chirality and to possess similar crystallographic orientation. Both correlations were found to decrease with increasing domain separation. Multiple nanocrystalline domains were grown in "molecule corrals", which are flat-bottomed, nanometer-sized pits produced on the graphite surface by an oxidation reaction. Domain structure was investigated using scanning tunneling microscopy (STM). The observations are explained as arising from anchoring interactions between the adsorbed monolayer and the liquid crystal interfacial fluid. A model based on a modification of the Rapini−Popoular potential for the surface free energy of a nematic LC is developed that quantitatively describes the orientational component of the interaction. From a statistical analysis of the STM data, it was possible to elucidate molecular-scale details of the interfacial LC fluid structure, including the orientation of the local LC director, the anchoring energy, and the way anchoring changed over different surface regions.

Introduction

The effect of substrate-induced bulk liquid crystal (LC) alignment forms the basis for many applications, including LC displays and LC-based storage media.[1] For this reason, understanding the relationship between the molecular-scale surface structure and bulk alignment in LC films is an important objective which has long been the focus of much attention.[2] It is known that molecular alignment in a preferred direction, or *anchoring*, can be induced by a suitable preparation of the substrate, for example, by rubbing, chemical treatment, or adsorption of an alignment layer such as a surfactant. Anchoring is the consequence of an elastic torque, exerted on the LC film by the surface, which tends to align the director along a preferred direction. Both short-range interaction at molecular length scales and long-range interaction at the macroscopic level are believed to play a role in determining the anchoring direction and strength of a surface.[3] Macroscopic-scale interactions include the effects of rubbing or scribing a surface, which tends to induce average molecular orientation parallel to the rubbing direction. In certain cases this tendency has been explained as arising from a coupling between the bulk LC elasticity and the surface topography.[4] Microscopic anchoring effects occur through van der Waals, electrostatic, and other noncovalent interactions, as well as through physical alignment arising from molecular-scale surface corrugation. The importance of these interactions is demonstrated by the sensitivity of bulk alignment to the chemical nature of the surface coating. If a surface is sufficiently smooth, molecular ordering in the first monolayer alone can determine alignment throughout the film.[5] The anchoring direction is very sensitive to the type of molecules in the alignment layer and their conformation and arrangement.[6−8]

Although widely studied, the problem of LC anchoring is far from solved. Many aspects of LC−surface interactions are poorly understood, particularly at microscopic length scales. Most studies of LC anchoring have employed a two-step procedure in which (1) a substrate is chemically or mechanically treated, followed by (2) application of a LC droplet and observation of the anchoring properties. In this type of system, the properties of the substrate are fixed during the processing which occurs in step 1. Thus, while the substrate may influence the alignment of the LC, the LC's influence on the substrate is negligible. In this paper we describe a different type of system in which a surface layer was deposited onto a substrate while it was in contact with a LC droplet. As a result, there existed a significant two-way interaction between the surface layer and LC fluid during the period that the surface layer was being formed. This interaction is reflected in the morphology of the surface layer, which shows a higher degree of long-range orientational and enantiomeric ordering than would be expected in its absence. By analyzing the structure of the surface layer with scanning tunneling microscopy (STM), we have been able to elucidate molecular-scale features of the LC−alignment layer interaction, including the anchoring energy, director alignment, and way the surface order parameter changes over different regions of the surface.

Our method is based on an analysis of the properties of the surface layer, from which certain details of the interaction with the LC are inferred. Although this approach does not provide direct information about the behavior of the LC in the interfacial

* To whom correspondence should be addressed. Phone: (801) 581−5383. E-mail: beebe@chemistry.chem.utah.edu.
[†] Western Washington University.
[‡] Harvard University.
[§] University of Utah.

10.1021/jp992142p CCC: $18.00
Published on Web 09/11/1999

CHART 1: 4′-Octyl-4-biphenylcarbonitrile (8CB)

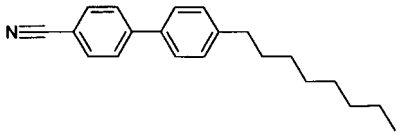

region, it does have one significant advantage: by studying the properties of the surface alignment layer, rather than the LC itself, it is possible to employ high-resolution microscopy, which enables connections to be drawn between the LC fluid structure and the molecular or submolecular details of the alignment layer. There is one further advantage. Conventional methods, such as polarization spectroscopy, contact angle measurements, and second-harmonic generation, provide information which reflects the average behavior of the LC−substrate interface over a macroscopic surface area.[9] By contrast, the method introduced here gives inherently local information, allowing one to investigate changes in anchoring behavior across a surface at very high lateral resolution.

In this paper we elaborate on the findings described in ref 10 and present new results regarding enantiomeric coupling interactions. The surface layer in our system is a crystalline monolayer of the same molecule forming the LC droplet. A monolayer nucleates and grows while in contact with a bulk LC droplet. After the monolayer has formed, its morphology is investigated with STM. Correlation between the orientations and other properties of adjacent microcrystalline domains seen in the STM images is attributed to an interaction of the monolayer with the LC film. A number of correlations were analyzed, two of which are discussed in detail. These involve chirality and domain orientation. Orientational correlations were analyzed using a statistical model to describe the orientational dependence of the LC−surface interaction energy and the local alignment of the LC director. Measurement of the dependence of this energy on domain size yields an estimate for the lateral (in-plane) persistence length of surface-induced ordering.

Experimental Section

The LC used in this study, 4′-octyl-4-biphenylcarbonitrile (8CB), is a room temperature bulk-phase smectic-A LC (Chart 1). The crystalline monolayer was grown on a substrate consisting of the basal plane of highly ordered pyrolytic graphite (HOPG) by placing a macroscopic droplet of the LC on the surface. STM has shown that a single crystalline monolayer forms, leaving the bulk of the droplet in a LC state.[11] The probe stylus penetrates through the bulk droplet to image just those molecules adsorbed to the graphite.

Molecules in the adsorbed monolayer organize into crystalline domains forming rowlike patterns. The size of these domains is typically restricted only by the size of the terrace on which they form (typically several μm^2 with the high-grade ZYA graphite used in this study). Rows are composed of approximately rectangular unit cells containing eight molecules arranged so that their dipoles cancel.[12] When 8CB adsorbs onto a surface, rotation about the C−C bond connecting the alkyl "tail" to the cyanobiphenyl "head" becomes strongly hindered. This rotational barrier imparts to the molecule a new chiral center; as a result crystalline 8CB films are chiral.

Molecular order in the crystalline monolayer reflects a balance between the competing influences of adsorbate−adsorbate, adsorbate−substrate, and adsorbate−LC interactions. In the absence of adsorbate−LC interactions, individual monolayer domains would be free to adopt any one of three energetically equivalent orientations, determined by the symmetry of the substrate, and either of two chiralities. The effect of interaction with the LC is to break this degeneracy by inducing a preferred alignment along the direction of the HOPG lattice vector that most closely matches the orientation of the LC director at that point. Another effect, which may be termed "enantiomeric correlation", was also observed. The effect produces a tendency for nearby surface domains to crystallize with similar chirality. It may also arise due to adsorbate−LC interactions.

Interaction between the surface layer and the bulk LC droplet was inferred by analysis of the relative crystalline properties of adjacent molecular domains in the surface layer. Multiple nanometer-sized domains were artificially produced using "molecule corrals", or etch pits in the basal plane of HOPG. Corrals were produced by heating freshly cleaved HOPG to 650 °C in air and afterward allowing it to cool before application of the liquid-crystal molecules.[13] This technique produces corrals which are uniformly circular and 3.35 Å deep (the spacing between graphite atomic layers). Analysis of orientational correlation was based on a total of 516 measurements taken from two samples, the first with corrals ranging in diameter from 100 to 250 nm, the second with diameters from 250 to 400 nm. Analysis of enantiomeric correlation was performed on a subset of these measurements. The effect of sample age was also examined and found to be inconsequential for the factors discussed in this paper over periods of up to two weeks. Tip perturbation could be ruled out or shown to be insignificant on the basis of three factors: (a) images are stable when continuously scanned over long periods of time, (b) image data are independent of the scan direction, and to a large extent insensitive to changes in tunneling current and bias voltage, and (c) different tips give comparable results. The analysis presented below assumes that molecular configurations in the corrals are at equilibrium. The best evidence we have to support the assumption of equilibrium conditions is that samples appear to be stable over periods of at least two weeks. A more rigorous test could be performed by examining the temperature dependence of the orientational correlation; however, such an experiment would be technically challenging, and we have not attempted it. All experiments were conducted at room temperature using mechanically cut Pt/Rh (80/20) tips with a homemade STM.[14]

Correlations in Domain Chirality

In previous studies we showed that molecules in the adsorbed monolayer crystallize by a nucleation-growth process, and that molecular ordering in each corral (growth) follows the formation of a separate nucleus.[15] In addition, it was shown that the rate of nucleus formation depends on corral area, rather than perimeter, indicating that nuclei form throughout the interior of the corral, and not just at the corral edges. Because the area of the terraces is generally so much larger than the area of corrals, molecules on the terraces always crystallize prior to molecules in the corrals, and therefore molecules in corrals always crystallize in the presence of an ordered terrace.

Figure 1 shows two molecule corrals, one containing disordered molecules (which are not molecularly resolved by STM due to their fast thermal diffusion[16]), and the second containing ordered molecules visible as rows. These corrals were closer together than was typical. Note that, in this case, the direction of the molecular rows within the second corral is different by ∼60° from the direction of the rows on the terrace. A histogram of a subset of intersection angles (Figure 2) reveals that only certain, discrete intersection angles are possible, determined by

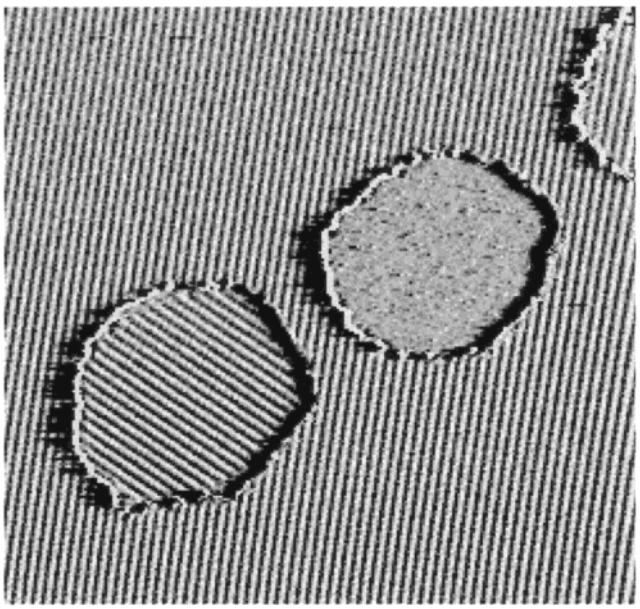

Figure 1. 2500 Å × 2500 Å constant-height STM image of two molecule corrals. The bright and dark rows on the terrace and in the bottom of one corral are crystalline arrays of adsorbed molecules. Typical imaging conditions were $V = -0.5$ to -1.0 V and $I = 1$ nA, and the ability to obtain an image such as this was not critically sensitive to these conditions. The corral which lacks these rows was filled with molecules in a disordered state, which diffuse too rapidly to resolve with STM (and not due to a lack of adsorbates): the sample is fully immersed in the LC droplet. The large heat of adsorption and the quasi-infinite flux of incoming adsorbates due to immersion guarantee this high adsorbate coverage. See ref 13.

the symmetry of the substrate and of the molecular rows. There is a large population of intersection angles at 0° not shown in Figure 2 (247 observations in this survey), whose position is indicated by the dashed line. These angles are similar to those reported in a study by Smith.[21]

The six observationally distinct possibilities are listed in Table 1 and shown schematically in Figure 3. This figure shows a corral surrounded by six molecular domains, one for each of the allowed orientations of 8CB on graphite. For compactness, the terrace and corral domains are represented with just two unit cells each, and six domains are shown occupying the terrace around the pit (separated by dashed lines). In an actual experiment, a single domain with thousands of unit cells would ordinarily occupy the entire terrace. Also, the molecules in the figure are drawn to a smaller scale than the graphite lattice, but rotational angles between domains and the arrangement of molecules within each domain are both accurate. Thus, the figure is highly schematic and is designed to illustrate the various angular possibilities.

We arbitrarily assign the three terrace domains in the left half of Figure 2 (L1, L2, and L3) as possessing left-handed chirality, and the three terrace domains on the right (R1, R2, and R3) as right-handed. The corral domain is also right-handed, and is oriented in the same direction as terrace domain R1. Members 2 and 3 of each set are related to member 1 of that set by a rotation of ±60°.

In all our studies of 8CB on HOPG, left-handed domains and right-handed domains have been observed with approximately equal frequency, indicating that the two "crystal enantiomers" are isoenergetic.[17] Furthermore, in all but the smallest corrals (radius ≤75 nm) we found no correlation between the terrace chirality and the corral chirality. However, in corrals smaller than about 75 nm, a correlation does appear to exist, becoming more pronounced with decreasing corral radius. The trend is for domains in small corrals to exhibit a statistical tendency toward homochirality with the terrace domain. This correlation is shown in Figure 4. The quantity F_o plotted along the ordinate is the fraction of corrals in which the chirality was opposite the surrounding terrace. A value of $F_o = 0.5$ corresponds to no net preference. This apparent correlation at small corral sizes was unexpected, since there is no obvious mechanism by which chiral information could be communicated between terrace and corral (in the bulk, 8CB is achiral). It is possible that crystallization in small corrals occurs by a mechanism different from that in larger ones which facilitates transmission of chiral information; however, we have no evidence for this. An alternative explanation, which is speculative, is that LC molecules near the solid interface, which are more ordered than those in the bulk, exhibit intramolecular mobility intermediate between the crystalline monolayer and bulk LC fluid. A related effect has been observed in computer simulations of thin alkane films, where mean molecular conformation depends on the distance of an alkane to the surface. Alkanes near the surface tend to adopt and maintain all-trans conformations, while those far from the surface exhibit more conformational freedom.[18,19] If rotation about the C−C bond connecting the cyanobiphenyl head to the alkyl tail in 8CB is partially hindered, and one molecular orientation is favored through interaction with the chiral monolayer, a statistical enantiomeric excess of the favored orientation could develop. Spontaneous formation of chiral domains in a bulk fluid LC composed of achiral molecules has recently been reported, an observation which supports this idea.[20] If similar chiral ordering occurred in the near-surface region of this system, the trend in Figure 4 would then be evidence for *enantiomeric* coupling between the surface and interfacial LC, a phenomenon which has not been previously reported. This coupling would be analogous to the orientational coupling between the surface and LC discussed below. The observed tendency for stronger enantiomeric correlation in small corrals would follow the same explanation developed below for the trend in orientational coupling.

Correlations in Domain Orientation

This section discusses the relative orientation of nearby crystalline domains. There is no unique way of defining the relative orientational angle between two molecular domains, just as there is no unique way of defining a unit cell for a crystal structure. In previous STM studies of 8CB, the intersection angle has normally been taken to be the angle between the molecular rows, because the rows appear so clearly pronounced in an STM image.[21] We adopt the same convention here, denoting intersection angles measured in this way with the symbol ϕ_I. However, we note that there is nothing special about this choice of definition; indeed, as shown below, the LC director does not align along the direction of the surface molecular rows, but rather aligns at an angle of ∼29°.

Measurements of the intersection angle of a large number of domains showed that each occurred with a different probability. Furthermore, the probability distribution depended on corral size, as shown in Figure 5. To analyze this size dependence, we divided the data into two sets, plotted separately in parts a and b of Figure 5. Figure 5a shows the alignment characteristics of molecules in corrals which possess the same chirality as that of the terrace; Figure 5b presents data for the cases where the corral chirality is opposite that of the terrace. The probability distribution plotted in the figures is therefore conditional on

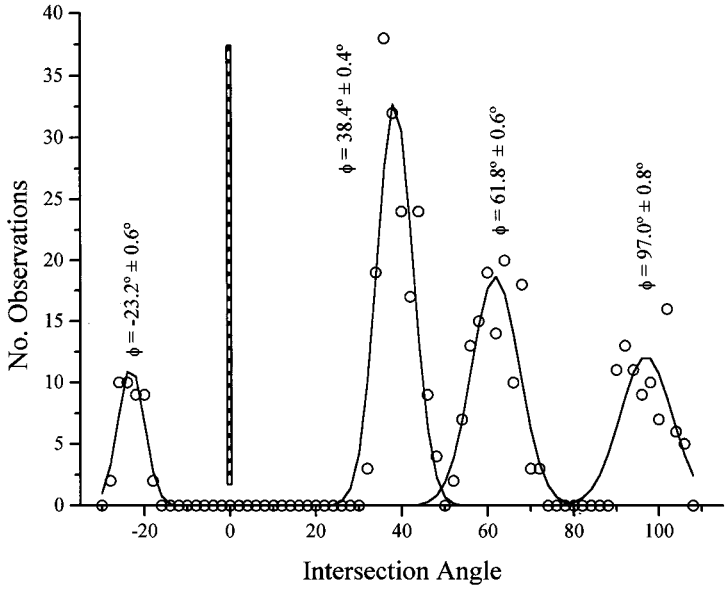

Figure 2. 8CB exhibits epitaxial growth on HOPG substrates, giving rise to discrete values in the intersection angles between adjacent crystalline domains. Six intersection angles are observed, four of which are shown in the histogram. Additional intersection angles which are observed but not shown occur at −61.8° and 0° (refer to the text).

TABLE 1: Observed Intersection Angles between Monolayer Domains in a Corral and on Its Adjacent Terrace Based on Several Hundred Observations, and the Persistence Length of Terrace−Corral Domain Interactions[a]

angle between corral and terrace domains in Figure 2	relative chirality between corral and terrace domains	ϕ_I (experimentally observed) (deg)	r^* (nm)
L1−corral	opposite	97.0 ± 0.8	36.0
L2−corral	opposite	38.4 ± 0.4	21.1
L3−corral	opposite	−23.2 ± 0.6	46.4
R1−corral	similar	0.0	
R2−corral	similar	61.8 ± 0.4	43.8
R3−corral	similar	−61.8 ± 0.4	43.8

[a] r^* is the distance at which the energetic cost of rotational misalignment decreases to $1.0kT$. Uncertainties were computed as $\pm\sigma/\sqrt{N}$, where σ is the standard deviation of the corresponding peak in Figure 2 and N is the number of observations of that intersection angle.

chirality (e.g., the open circles in Figure 5a show the experimentally measured probability of observing the intersection angle $\phi_I = 0°$, given that the chirality of the corral domain is the same as the terrace domain).

The intersection angles $\phi_I = +61.8°$ and $\phi_I = -61.8°$ were found to occur with nearly equal frequency. Therefore, in subsequent experiments we did not distinguish between these two angles, and so in Figure 5a the set of points labeled $\phi_I = 61.8°$ actually contains observations of both $\phi_I = 61.8°$ and $\phi_I = -61.8°$. In Figure 2 these two angles have been combined and are shown plotted together. Because the correlation seen in Figure 4 occurs in only the smallest corrals, we have neglected this effect in the analysis of the next section.

The points plotted in Figure 5 show a remarkable dependence of the orientation of corral domains on the orientation of the surrounding terrace domain. The data fall naturally into two sets, with the intersection angles $\phi_I = 0°$ and $\phi_I = 38.4°$ being strongly preferred at small corral sizes. As corral size increases, this preference diminishes, although a significant preference exists even for corrals over 150 nm in radius.

What is the cause of the observed correlation? We interpret this preference as evidence of an orientation-dependent interaction between corral and terrace molecules. The corral domain, which always nucleates and grows long after the terrace domain is fully formed, appears to experience an energetic bias, causing it to align with the terrace domain. To understand this behavior, we note that the orientation of molecules within a corral is

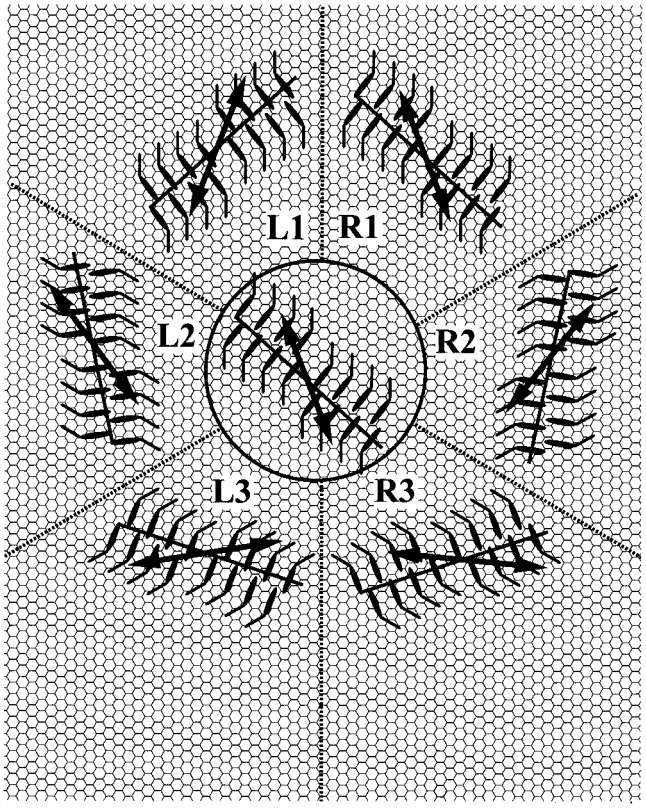

Figure 3. 8CB molecules on HOPG crystallize in two chiral unit cells, which adopt three observationally distinct orientations. Each unit cell contains eight molecules, arranged so that the dipole moment of the cyanobiphenyl heads mutually cancel. Parts R1, R2, and R3 show small portions of right-handed domains in three different orientations. Parts L1, L2, and L3 show left-handed domains. The central part of the figure shows a portion of a domain in a molecule corral. Normally a single crystalline domain would occupy the entire terrace. Here six terrace domains have been shown together for illustrative purposes. The solid black lines give the direction of the molecular rows prominently observed in STM images. The arrows indicate the preferred orientation of the LC director above each domain. Note that the molecule figures are drawn to a smaller scale than the graphite substrate.

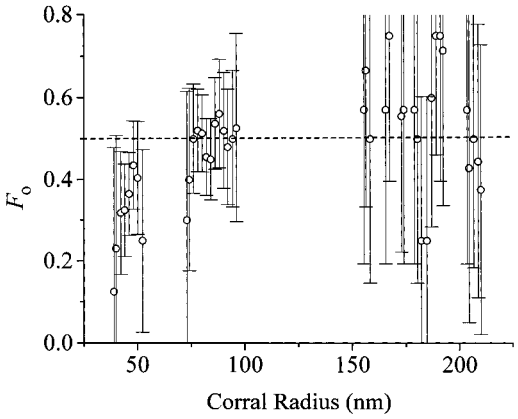

Figure 4. In small corrals, there is a tendency for corral domains to adopt the same chirality as the terrace domain. The quantity F_o is the fraction of corrals with chirality opposite that of the surrounding terrace.

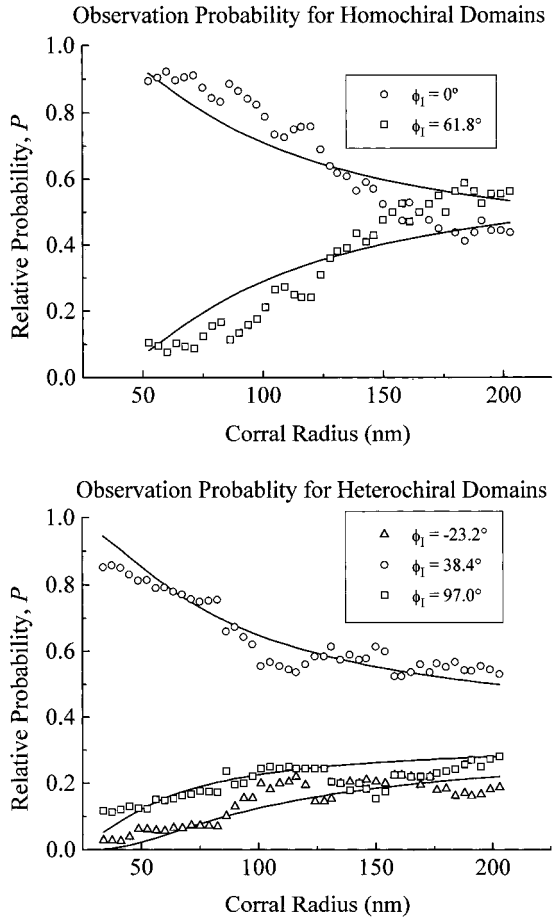

Figure 5. Conditional probability $P(R,\phi_I)$ of observing various intersection angles, if the corral and terrace domains possess (a, top) the same chirality and (b, bottom) different chiralities. The probability distribution depends strongly on corral size, shown on the abscissa. Solid lines are a fit of the interaction model described by eq 2 to the experimental data (see the text).

effectively determined at the time of nucleus formation since the energetic cost of domain rotation after nucleation in a corral is too large to permit it to occur after the nucleation event. The observed dependence of domain alignment on corral radius can therefore be qualitatively understood by the fact that nuclei form in the interior of corrals, so that the average distance of a nucleus in a corral to molecules on the terrace increases with corral size, and hence the average orientational interaction decreases with increasing corral size.

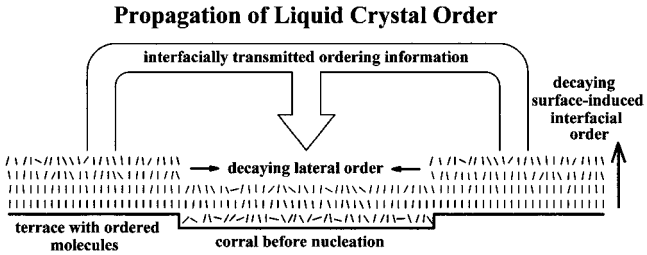

Figure 6. Schematic illustration of LC-induced surface alignment. Rods represent ordering of liquid crystal molecules in the interfacial region above the surface. The orientation of the rods is not intended to suggest that the molecules are aligned with their long axes perpendicular to the surface plane, but instead to represent some degree of order which is transmitted laterally.

By what mechanism is the conjectured interaction between corral and terrace domains transmitted? We rule out a direct interaction between corral and terrace molecules on the basis of dispersive and inductive interactions because these forces are much too short ranged to act over the distances indicated in Figure 5. Although the polar molecules used in this study might suggest that electrostatic interactions are the cause, other reasons allow us to rule this choice out as well: The symmetry of the unit cell results in a mutual cancellation of the molecular dipoles. As a result, the lowest-order nonzero electrostatic term arises from quadrupole−quadrupole interactions, which are short ranged and comparatively weak.

To provide some insight into the magnitude of the energies involved, and to validate our ruling out of these interactions, we give an order-of-magnitude estimation of the interaction energy of two identical, fixed, polarizable, rodlike molecules separated by a distance $r = 100$ nm, interacting through a vacuum. Neglecting all angular-dependent terms in the interaction energy expression[22] and taking only the lowest order term in r gives

$$U_{\text{electrostatic}} \approx \mu^2/4\pi\epsilon_o r^3 \approx 10^{-9} kT \quad (1a)$$

$$U_{\text{dispersion}} \approx 3I\alpha^2/2(4\pi\epsilon_o)^2 r^6 \approx 10^{-14} kT \quad (1b)$$

$$U_{\text{induction}} \approx \mu^2\alpha/2(4\pi\epsilon_o)^2 r^6 \approx 10^{-16} kT \quad (1c)$$

where $\mu \approx 10^{-30}$ C m is the static dipole moment, $I \approx 10^{-18}$ J is the first ionization energy, $\alpha \approx 10^{-39}$ C^2 m^2 J^{-1} is the dipole polarizability, $\epsilon_o = 8.5 \times 10^{-12}$ C^2 J^{-1} m^{-1} is the dielectric permittivity of free space, and $kT \approx 10^{-21}$ J is the amount of thermal energy available at 300 K. The above expression for the electrostatic energy is for a pair of interacting static dipoles. The interaction energy of two quadrupoles would be even smaller. We conclude from these estimated energies that electrostatic, inductive, and dispersion interactions are many orders of magnitude too small to account for the observed orientational preference acting over the distances shown in Figure 5.

An alternative and more plausible explanation of the data in Figure 5 comes from considering the effect of surface-induced ordering of LC molecules in the interfacial region. The interaction of ordered molecules in the adsorbed monolayer with molecules in the LC fluid immediately above them could provide a mechanism for transmission of orientational information over much longer distances than is possible with the kinds of "through-space" interactions discussed above. Figure 6 illustrates schematically how this could be accomplished. Adsorbate molecules on the terrace, which order prior to those in the corral,

produce local orientational ordering of the LC fluid above them. Because this molecule is a liquid crystal in the bulk, this order extends some length over the edges of the corrals, decaying with increasing distance from the molecules on the terrace. The orientational correlation could then arise from the interaction between oriented molecules in the interfacial liquid-crystalline region and nuclei forming within corrals (see Figure 6).

For most LC films in contact with a solid surface, bulk-induced surface ordering is not believed to be important since the coupling energy between an adsorbed LC molecule and the surface is generally so much larger than the coupling energy with the bulk fluid.[24] However, in systems where the surface layer can adopt more than one isoenergetic orientation (i.e., when the system displays degenerate anchoring), even weak coupling with an orientational influence such as the bulk LC film may produce a measurable orientational preference. The graphite substrates used in this study possess 6-fold rotational symmetry, and in the absence of an external influence, crystalline 8CB domains are free to adopt any one of several isoenergetic orientations. In this case, even a very small energetic bias favoring one orientation over the others would produce a shift in the distribution.

To further quantify the nature of the interaction, we fit the data in Figure 5 using an orientational interaction potential based on a modification of the Rapini−Popoular potential for the surface free energy of a nematic LC.[25] The potential was constructed as follows: We conjectured that alignment of a protonucleus at position $\bar{r}$ in a corral should be proportional to the autocorrelation function between director alignment at $\bar{r}$ and over the terrace: $U(\bar{r}) \propto S(\bar{r}) = \langle f(\bar{r})\, f(\bar{r}_{\text{terrace}})\rangle$, where angular brackets denote a spatial and thermal average. We postulated that the director gradually changes moving away from the terrace toward the center of the corral, causing $S(r)$ to diminish; the LC fluid gradually loses its "memory" of terrace-induced alignment. An exponential function was found to adequately describe this effect.

We postulate that $S(\bar{r})$ gradually changes as one moves toward the center of the corral, away from the terrace. As shown below, this change is found to be in the form of a gradual decay, indicating that the LC fluid slowly loses its memory of the terrace-induced alignment. An exponential decay function was found to adequately describe this effect, which was chosen by analogy to the situation observed for surface-induced layering in nematic LCs, where the decay occurs exponentially along the surface normal.[26] We emphasize however that the data do not allow us to preclude other decay functions; for example, it was found that a power-law decay gave comparable results within the uncertainty range given by the scatter in the data.

We assume that both the ordered terrace and protonucleus induce a local preferred LC anchoring, and that when the two anchoring directions coincide, the orientational energy is minimized. We denote the difference between the terrace and protonucleus anchoring directions as ϕ_A. ϕ_A is related to the STM data in the following way: Let ϕ_o be the offset angle between the molecular surface rows and the local preferred orientation of the LC director. In ref 10, we studied 8CB films deposited in the presence of a strong magnetic field and found that the sign of ϕ_o depended on the surface layer's chirality, with ϕ_o being negative for right-handed chirality and positive for left-handed chirality. Then a geometrical analysis shows that $\phi_A = \phi_I - 2(\delta_{CT} - 1)\phi_o$, where ϕ_I is the intersection angle between terrace and corral molecular rows in the STM images, and δ_{CT} is the Kronecker δ function ($\delta_{CT} = 1$ when the corral and terrace domains are homochiral and 0 when they are heterochiral).

The final element of the model is the introduction of a coupling constant, W. W is the surface anchoring energy, which describes the strength of the orientational dependence of the interfacial tension between a LC film and an aligning substrate. LC−substrate systems with large anchoring energies exhibit stronger preferential alignment than those with small anchoring energies.

Combining these ideas, we arrive at the following expression for the orientational free energy U of a protonucleus located a distance r from the corral edge:

$$U(r,\phi_I) = S_o(W/2)\sin^2\phi_A e^{-kr} \tag{2}$$

where S_o is the value of $S(\bar{r})$ at the corral's perimeter and k is a decay constant. The divisor of 2 is included to provide consistency with the Rapini−Popoular definition of the anchoring energy.

Using the energy function in eq 2, and assuming an equilibrium distribution of intersection angles, the probability that a protonucleus which forms at a distance r from the edge of a corral will orient at an angle ϕ_I with respect to the molecules on the terrace is

$$P(r,\phi) = \frac{\exp[-U(r,\phi_I)/kT]}{\sum_{\phi}\exp[-U(r,\phi_I)/kT]} \tag{3}$$

Since nuclei can form almost anywhere within a corral, it is necessary to average $P(r,\phi_I)$ over the entire corral to get the probability $P(R,\phi_I)$ of observing the angle ϕ_I in a corral with radius R. Here we make another assumption, that protonuclei cannot form closer to the corral edge than a certain distance d. This assumption is motivated by the experimental observation that molecules near corral edges (both on the terrace and in the corral) appear to be inherently less well-ordered than molecules which are far from a step edge. This reduction in surface order results in an enhanced degree of molecular mobility, causing STM images of molecules near corral edges to appear "blurred". A second reason for introducing this parameter comes from an analysis of the corral size dependence of nucleation rates given in ref 13. This study indicated that nuclei are inhibited from forming very close to corral edges. The average $\langle P(r,\phi)\rangle_r = P(R,\phi)$ is found by integrating eq 3 over the interval $r = d$ to R, and dividing by the corral's effective area, $\pi(R - d)^2$.

$$P(R,\phi_I) = \frac{1}{\pi(R-d)^2}\int_d^R 2\pi r P(r,\phi_I)\,dr \tag{4}$$

The solid lines in Figure 5 are the result of a least-squares fit of the experimental data using the probability distribution function in eq 4 and the effective interaction potential in eq 2. All of the data shown in Figure 5 fit simultaneously using a quasi-Newton optimization algorithm. The probability function was integrated numerically to high precision using an implementation of the algorithm QAGS described in ref 26.

There are five data sets in Figure 5, one for each of the intersection angles $\phi_I = 0.0°$, $-23.2°$, $38.4°$, $61.8°$, and $97.0°$. Each of these was found to be satisfactorily fit by a single set of model parameters. These were $W = (4.6 \pm 0.3) \times 10^{-19}$ J, $k = (8.6 \pm 0.4) \times 10^{-4}$ nm^{-1}, $\phi_o = 28.9 \pm 0.9°$, and $d = 10$ nm.[27] Boundary conditions dictate that $S_o = 1$ in the analysis. Initially, we developed a fitting routine which iteratively adjusted

each of the four variables $\{W, k, \phi_o, d\}$ simultaneously in an attempt to generate the best least-squares fit to the data in Figure 5. However, the optimization algorithm proved insufficiently robust to reliably converge on a single solution, making it necessary to constrain the value of one parameter, d, while varying the remaining three. Using this approach, the analysis was repeated with a number of different values of d over the range $d = 0-25$ nm. All choices gave very similar values for the total error ϵ computed by the fitting routine, where ϵ is the square root of the sum of the squares of the differences between the points in the experimental probability distribution plotted in Figure 5 and the values predicted by the model. The overall quality of the fit was thus insensitive to the choice of d, making it impossible to arrive at a reliable estimate for this parameter working solely from a least-squares analysis of the data. Instead d was estimated on the basis of the expectation that it should approximate the width of the disordered region seen in STM images of 8CB films near corral edges. On the basis of the results described in ref 13 and measurements of STM images collected as part of the present study, this width is ~10 nm. Changes in d by as much as ±5 nm around this value had little effect on the least-squares best-fit values of the other parameters.[28] We now comment on the remaining model parameters.

The physical meaning of the anchoring energy is illustrated by an example. Focusing on the two homochiral intersection angles $\phi_I = 0.0°$ and $\phi_I = 61.8°$, we find the energy difference between two protonuclei aligned at these angles, each located 10 nm from the corral edge, to be $\Delta U = 8.4$ kJ mol^{-1}. If the two nuclei were located closer to the corral center, this energy difference would be smaller. Since the only difference between these two protonuclei is their orientational alignment, their interaction energy with substrate and the intermolecular interaction energy between the molecules within the protonucleus are both *identical*. Hence, the relative probability of observing these two angles must arise entirely from differences in their interaction with the LC fluid above them. This difference is $\Delta U = 8.4$ kJ mol^{-1}, with the protonucleus aligned at 0.0° interacting more favorably with the LC fluid than the one aligned at 61.8°.

We have equated the model parameter W with the surface anchoring energy. Anchoring energies are typically expressed as an energy per unit area, and are usually observed to fall within the range[28] $10^{-7}-10^{-3}$ J m^{-2}. It is instructive to compare this range of values to the strength of the coupling constant determined here. Dividing W by the surface area of a protonucleus gives a consistent basis for comparison. The actual size of a protonucleus is unknown, but must lie in the range $1a$ to $200a$, where a is the area of a single unit cell in the crystalline monolayer[16] ($a = 11$ nm^2). The upper size limit is estimated from the area of the smallest corral in which a crystalline monolayer has been observed to form (diameter ~50 nm). Dividing by this range of areas gives the orientational interaction energy per unit area of a protonucleus with the LC film, $10^{-7}-10^{-5}$ J m^{-2}. Normalized in this way, the anchoring energy found in this study is similar to anchoring energies measured by traditional means.

The second model parameter is $\phi_o = 28.9°$. As discussed in ref 10, it represents the preferred angle between the direction of the molecular rows in the crystalline monolayer and the surface projection of the orientation of the LC director. In the reference cited, the orientation of the local LC director relative to the surface rows was independently established in a separate experiment and was found to equal, or nearly equal, the value ϕ_o. The projection of the director above the corral domain is indicated in Figure 2 by an arrow. Interestingly, the director does not coincide with the orientation of molecules in the surface layer; this result is anticipated by the trend in Figure 5, which shows that the preferred orientation between heterochiral domain pairs ($\phi_1 = 38.4°$) is not one which most closely coaligns molecules. Although not directly measured in this study, it is evident from the existence of the orientational correlation that the LC fluid must exhibit either planar or tilted anchoring, since homeotropic anchoring would give the fluid C_∞ symmetry about the surface normal, and hence no basis could exist for communicating a preferred in-plane alignment to the monolayer.

The last model parameter is the decay constant, k. It describes the rate of decay of the magnitude of the order parameter $S(\bar{r})$ with distance from a corral's edge. The quantity $k^{-1} = 11.6$ nm is a characteristic length scale defining the range of the interaction. It represents the persistence length of terrace-induced LC fluid ordering in a direction parallel to the surface, $\xi_{||}$. An alternative, perhaps more physically intuitive measure of the decay length is the distance r^* at which the energetic cost of rotational misalignment for a protonucleus decreases to kT. This distance is given in Table 1 for each intersection angle at $T = 300$ K. The range of the interaction determined this way, 21.1−46.4 nm, is qualitatively consistent with expectation, on the basis of the distance scale in Figure 5. Note that there is no energetic cost at any distance associated with the intersection angle $\phi_I = 0$, since this angle represents perfect alignment of the corral and terrace domains. An energy difference as small as $1.0kT$ would produce a 73% excess of the favored orientation in a two-state system. When a bulk LC is far-removed from a transition temperature, transverse autocorrelations in the director arising from thermal fluctuations formally decay as r^{-1}, with a correlation length on the order of 1 nm.[30] We observe correlations over a significantly larger distance, following a decay profile inconsistent with thermally induced disordering. This suggests that anchoring plays a dominant role in stabilizing long-range LC order near the interface, and that thermal fluctuations are of secondary importance here.

We now offer a tentative explanation as to why $S(\bar{r})$ decays moving away from a corral edge, toward the center. The explanation is based on the observation made long ago that different surfaces or surface treatments can induce different alignments in the same LC. For example, 8CB molecules in films deposited onto water,[31] glass, or glass coated with silane surfactants[32] prefer to orient with their long axis directed perpendicular to the surface plane, whereas rubbed glass or rubbed silane-coated glass[33] induces 8CB molecules to align with their axis parallel to the surface plane. Furthermore, Shen's group has shown that, on smooth, flat surfaces, a single monolayer is sufficient to determine the orientation of LC molecules throughout the bulk film.[34] On the basis of these general observations, it is possible that the terrace surface, which is covered by a crystalline monolayer of 8CB, induces a *different* anchoring of the LC fluid above it than does an as-yet uncrystallized corral surface. It is not necessary to know how the two surfaces differ in their preferred alignments, since any difference would produce a decay in $S(\bar{r})$ (which represents *terrace*-induced order). To see why this is so, consider the hypothetical example of surface-induced LC ordering shown in Figure 7. In this example the LC fluid alignment induced by the terrace differs by 90° from that induced by the corral. The local alignment of LC fluid molecules is represented by a series of planes which change orientation by 90° in going from the terrace to the corral. Crystallized molecules on the terrace are represented as a set of parallel lines. It is clear from the figure that the fluid's memory of the terrace will decay with increasing

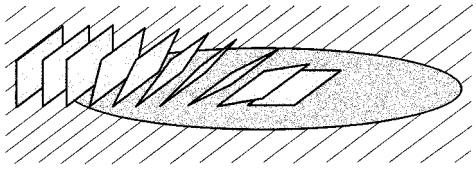

Figure 7. If the terrace and corral surfaces tend to induce different anchoring of the LC interfacial fluid, then the degree of terrace-induced ordering in the fluid would decay with increasing distance from the corral edge. The plane objects are not meant to imply any particular orientation of the LC molecules, but rather to suggest a change in their preferred orientation with position.

distance from the corral's edge. Furthermore, there will be an unavoidable discontinuity in the LC at the center of the corral where planes from different directions (not shown) meet. These conclusions hold true for any reasonable surface-induced ordering; as long as the LC molecules above the corral prefer to adopt a different orientation than those above the terrace, the terrace-induced LC ordering will decay, and there will be a discontinuity at the corral's center.

To our knowledge, the orientation of LC molecules immediately above the surface has never been measured in this system, although such a measurement could be very illuminating. To test the hypothesis put forward in the previous paragraph, one would need to make two measurements, one above a crystallized surface, and one above an uncrystallized surface. The second measurement is made difficult by the fast nucleation rate of 8CB at room temperature, which leads to fully crystallized terraces in a matter of seconds near room temperature. Increasing the temperature to just below the smectic → nematic transition temperature (33.5 °C) would decrease the nucleation rate substantially, possibly enough to make the determination feasible,[15] but also introducing additional temperature-induced order differences.

Conclusions

Structural correlations between monolayer domains trapped in molecule corrals and domains on the surrounding terrace have been studied by STM. Relationships were observed between the chirality and orientation of adjacent domains, with homochirality and the intersection angles $\phi_I = 0°$ and $\phi_I = 38.4°$ being preferred in small corrals. Both preferences were found to diminish in larger corrals. To explain the correlations, a model was proposed on the basis of a postulated interaction of the terrace and corral domains with the interfacial LC fluid. While the explanation is qualitative with respect to describing enantiomeric correlations, it was shown that the orientational data were uniformly and quantitatively described using a model for surface anchoring based on a modified form of the Rapini−Popoular potential. A fit to the experimental data indicated that the LC director preferentially aligns at an angle of 28.9° with respect to the molecular rows, providing a direct connection between the molecular-scale details of the alignment monolayer and the orientational properties of the interfacial LC fluid. The analysis showed that terrace-induced orientational ordering of the LC fluid exhibits exponential decay as one moves away from a corral edge with a correlation length of $\xi_{||} \approx 11.6$ nm. The anchoring energy was found to have a value of 4.6×10^{-19} J.

These findings are significant for the information they provide about the interaction between a LC and a surface layer at nanometer length scales. An understanding of such interactions is critical for the tailored design of new alignment layer preparations. Recent advances in methods for nanoscale surface chemical patterning hold promise for enabling a new generation of LC devices based on substrates whose LC anchoring characteristics vary over submicrometer length scales.[34−36] The success of this technology will require an improved understanding of the microscopic aspects of LC anchoring, and the manner in which anchoring changes over small length scales in response to variations in substrate properties. This understanding in turn will require new methods for performing localized measurements of film and fluid structure, with the present combined experimental and theoretical procedure being an example.

Acknowledgment. This work was supported by the National Science Foundation (NSF CHE9357188), the Camille and Henry Dreyfus Foundation, the Alfred P. Sloan Foundation, and Western Washington University. Discussions with Forrest Stevens are acknowledged with thanks.

References and Notes

(1) Jerome, B. *Rep. Prog. Phys.* **1991**, *54*, 391.
(2) Mauguin, C. *C. R. Acad. Sci.* **1913**, *156*, 1246.
(3) Chen, W.; Feller, M. B.; Shen, Y. R. *Phys. Rev. Lett.*, **1989**, *63*, 2665.
(4) Berreman, D. W. *Phys. Rev. Lett.* **1972**, *28*, 1683.
(5) Johannsmann, D.; Zhou, H.; Sonderkaer, P.; Wierenga, H.; Myrvold, B. O.; Shen, Y. R. *Phys. Rev. E* **1993**, *48*, 1889. Zhuang, X.; Marrucci, L.; Shen, Y. R. *Phys. Rev. Lett.* **1994**, *73*, 1513.
(6) Gibbons, W. M.; Shannon, P. J.; Sun, S. T.; Swetlin, R. J. *Nature* **1991**, *351*, 49.
(7) Crawford, G. P.; Ondris-Crawford, R.; Zumer, S.; Doane, J. W. *Phys. Rev. Lett.* **1993**, *70*, 1838.
(8) Zhu, Y.-M.; Lu, Z.-H.; Xia, X. B.; Wei, Q. H.; Xiao, D.; Wei, Y.; Wu, Z. H.; Hu, Z. L.; Xie, M. G. *Phys. Rev. Lett.* **1994**, *72*, 2573.
(9) Sonin, A. A. *The Surface Physics of Liquid Crystals*; Gordon and Breach: Amsterdam, 1995.
(10) Patrick, D. L.; Cee, V. J.; Baker, R. T.; Beebe, T. P.; Jr. Manuscript submitted for review.
(11) Foster, J. S.; Frommer, J. E. *Nature* **1988**, *333*, 542.
(12) Patrick, D. L.; Beebe, T. P. Jr. *Langmuir* **1994**, *10*, 298 and references therein.
(13) Patrick, D. L.; Cee, V. J.; Beebe, T. P. Jr. *Science* **1994**, *265*, 231.
(14) Zeglinski, D. M.; Ogletree, D. F.; Beebe, T. P. Jr.; Hwang, R. Q.; Somorjai, G. A.; Salmeron, M. B. *Rev. Sci. Instrum.* **1990**, *61*, 3769.
(15) Patrick, D. L.; Cee, V. J.; Beebe, T. P. Jr. *J. Phys. Chem.* **1996**, *100*, 8478.
(16) Patrick, D. L.; Cee, V. J.; Purcell, T. J.; Beebe, T. P. Jr. *Langmuir* **1996**, *12*, 1830.
(17) Stevens, F.; Dyer, D. J.; Walba, D. M. *Angew. Chem.* **1996**, *35*, 900.
(18) Xia, T. K.; Ouyang, J.; Ribarsky, M. W.; Landman, U. Phys. *Rev. Lett.* **1992**, *69*, 1967.
(19) Patrick, D. L.; Purnell, B.; Ladd, L. Unpublished results.
(20) Link, D. R.; Natale, G.; Shao, R.; Maclennan, J. E.; Clark, N. A.; Korblova, E.; Walba, D. M. *Science* **1997**, *278*, 1924.
(21) Unit cells of 8CB on graphite occur in two chiral forms, related to one another by reflection symmetry. The two forms are energetically degenerate, and all unit cells within a given domain are invariably of the same chirality. For details refer to the paper by D. P. E. Smith (*J. Vac. Sci. Technol.* **1991**, *B9*, 1119), where the term "helicity" is used.
(22) Buckingham, A. D. In *Intermolecular Interactions: From Diatomics to Biopolymers*; Pullman, B., Ed.; John Wiley & Sons: New York, 1978; pp 1−67.
(23) Israelachvili, J. *Intermolecular and Surface Forces*; Academic Press: New York, 1992.
(24) Brown, G. H.; Doane, J. W. *Appl. Phys.* **1974**, *4*, 1.
(25) Rapini, A.; Popoular, M. J. *J. Phys. (France) Colloq.* **1969**, *30*, C4−54.
(26) Piessens, R.; deDoncker-Kapenga, E.; Uberhuber, C. W.; Kahaner, D. K. *QUADPACK*; Springer-Verlag: New York, 1983.
(27) Uncertainties in the fitted parameters are reported as $\pm 1\sigma$, where the standard deviation σ was computed from the curvature of the error surface in the neighborhood of the minimum: $\sigma_x = [\partial\chi^2/\partial z^2]^{-1/2}$; $\chi^2 = \sum_i (f_i - f_i)^2$.
(28) The fitting procedure was repeated several times for each choice of d, initiated from widely spaced points in the other parameter space dimensions. Each time the minimizer converged to the same solution,

offering some assurance that the best-fit values represent the true global minimum on the error hypersurface.

(29) Yokoyama, Y. *Mol. Cryst. Liq. Cryst*. **1988**, *165*, 265.

(30) de Gennes, P. G.; Prost, J. *The Physics of Liquid Crystals*, 2nd ed.; Clarendon Press: Oxford, 1993.

(31) Guyot-Sionnest, P.; Hsiung, H.; Shen, Y. R. *Phys. Rev. Lett*. **1986**, *57*, 2963.

(32) Mullin, C. S.; Guyot-Sionnest, P.; Shen, Y. R. *Phys. Rev. A* **1982**, *39*, 3745.

(33) Chen, W.; Feller, M.; Guyot-Sionnest, Y. R., P.; Mullin, C. S.; Hsiung, H.; Shen, Y. R. Photochemistry in Thin Films. *SPIE* **1989**, *104*, 1056. Chen, W.; Feller, M.; Shen, Y. R. *Phys. Rev. Lett.* **1989**, *63*, 2665.

(34) Johannsmann, D.; Zhou, H.; Sonderkaer, P.; Wierenga, H.; Myrvold, B. O.; Shen, Y. R. *Phys. Rev. E* **1993**, *48*, 1889. Feller, M. B.; Chen, W.; Shen, Y. R. *Phys. Rev. A* **1991**, *43*, 6778.

(35) Wang, D.; Thomas, S. G.; Wang, K. L.; Xia, Y.; Whitesides, G. M. *Appl. Phys. Lett*. **1997**, *70*, 1593.

(36) Gupta, V. K.; Abbott, N. L. *Science* **1997**, *276*, 1533.